Journal of Cellular Biochemistry 100:326–338 (2007)

Nanotopographical Stimulation of Mechanotransduction and Changes in Interphase Centromere Positioning

Matthew J. Dalby,[1]* Manus J.P. Biggs,[1] Nikolaj Gadegaard,[2] Gabriela Kalna,[3] Chris D.W. Wilkinson,[2] and Adam S.G. Curtis[1]

[1]Division of Infection and Immunity, Centre for Cell Engineering, Joseph Black Building, Institute of Biomedical and Life Sciences, University of Glasgow, Glasgow G12 8QQ, Scotland, United Kingdom
[2]Department of Electronics and Electrical Engineering, Centre for Cell Engineering, Rankine Building, University of Glasgow, Glasgow G12 8QQ, Scotland, United Kingdom
[3]Department of Mathematics, University of Strathclyde, Livingstone Tower, 26 Richmond Street, Glasgow G1 1XH, Scotland, United Kingdom

Abstract We apply a recently developed method for controlling the spreading of cultured cells using electron beam lithography (EBL) to create polymethylmethacrylate (PMMA) substrata with repeating nanostructures. There are indications that the reduced cell spreading on these substrata, compared with planar PMMA, results from a reduced adhesivity since there are fewer adhesive structures and fewer of their associated stress fibres. The reduced cell spreading also results in a reduced nuclear area and a closer spacing of centrosomes within the nucleus, suggesting that the tension applied to the nucleus is reduced as would be expected from the reduction in stress fibres. In order to obtain further evidence for this, we have used specific inhibitors of components of the cytoskeleton and have found effects comparable with those induced by the new substrata. We have also obtained evidence that these subtrata result in downregulation of gene expression which suggests that this may be due to the changed tension on the nucleus: an intriguing possibility that merits further investigation. J. Cell. Biochem. 100: 326–338, 2007.

Key words: mechanotransduction; cytoskeleton; interphase nucleus organization; nanotopography; nanobioscience

Direct mechanotransduction from the extracellular matrix, that is force transmission to the cell nucleus, has clear roles in regulation of blood pressure, vascular response to fluid shear stress, bone remodelling, maintenance of muscle and perception of touch and sound [Katsumi et al., 2004] to name a few.

There are presently two main theories on how the cell may relay mechanical signals from the plasma membrane. Firstly, is Ingber's [1993, 2003a,b] theory of tensional integrity (tensegrity). The theory of tensegrity is derived from civil engineering principles, whereby a structure is stabilized through continuous tension, rather than compression [Fuller, 1961]. Ingber's tensegrity units use microfilaments (MFs) and microtubules (MTs), with MTs acting as load bearers and the MFs under tension. In this model, intermediate filaments (IFs) also act in a tensile mode and are associated with MT stabilisation. In order to have a tensegrity structure, prestress is required. It is likely that actin/myosin motors in cortical and contractile stress fibres anchored to focal adhesions are used to apply prestress to the tensegrity structure; acting like cellular guy wires. A variation on this has been proposed, whereby IFs form the tensile element of the tensegrity structure [Charras and Horton, 2002].

Biophysical data backs up both theories. In vitro, studies with isolated MFs and MTs showed MFs to be better at withstanding

Grant sponsor: BBSRC David Phillips Fellow; Grant sponsor: Royal Society of Edinburgh Research Fellow; Grant sponsor: EC; Grant number: NANOCUES NMP-STREP 2004 505868-1.

*Correspondence to: Matthew J. Dalby, Division of Infection and Immunity, Centre for Cell Engineering, Joseph Black Building, Institute of Biomedical and Life Sciences, University of Glasgow, Glasgow G12 8QQ, Scotland, UK. E-mail: M.dalby@bio.gla.ac.uk

Received 23 February 2006; Accepted 19 May 2006
DOI 10.1002/jcb.21058

tension and MTs to be better at withstanding compression [Mizushima-Sugano et al., 1983]. Also, when isolated, MTs are straight (bent in living cells as if under compression), MFs are bent (straight in living cells as if under tension) and IFs are entangled (merely bent in living cells as if under tension) [Hotani and Miyamoto, 1990; Janmey, 1991; MacKintosh et al., 1995]. These observations are consistent with engineering rules stating that tension straightens and compression bends.

The second model is given by Forgacs [1995], Shafrir and Forgacs [2002] who adapts percolation theory. This also relies on an interconnected cytoskeletal network. However, percolation simply relies on enough cytoskeleton interconnection to allow propagation of signals to the nucleus; this is called the critical concentration.

A separate theory of interest to us is that of consistency of interphase chromosomal positioning. It has been proposed that rather than the chromosomes (Chs) being randomly arranged during interphase, that there is, in fact, a consistency of position [Heslop-Harrison et al., 1993; Heslop-Harrison, 2000, 2003]. In fact, an emerging theory is that of Chs occupying discrete territories within the nucleus (Cremer and Cremer [2001] have written an in-depth review on this).

A number of early investigators observed filaments (possibly of DNA) connecting interphase Chs [DuPraw, 1965; Hoskins, 1965, 1968]. Later, Fey et al. [1984] showed that in interphase cells, the nuclear matrix appears to interconnect different nuclear components, such as nucleoli, to each other and the surrounding cytoskeleton. More recently, it has been shown that the human endothelial cell genomes behave as a continuous, elastic structure [Maniotis et al., 1997a,b].

Further to this, there have been a number of reports on spatial organisation within chromosomes in the interphase nuclei. These include the major histocompatibility complex on Ch 6 [Volpi et al., 2000] and the epidermal differentiation complex on Ch 1 [Williams et al., 2002].

In order to investigate and link these theories, this report uses nanotopography as a non-invasive tool to alter mechanotransduction in human fibroblasts; representing changes in matrix morphology. The nanotopography used was fabricated by electron beam lithography (EBL). The surface used (hex, 120 nm diameter, 300 nm spaced pits with hexagonal arrangement) has been shown to have an inhibitory effect on the spreading and cytoskeletal organisation of this cell type [Dalby et al., 2004b].

MATERIALS AND METHODS

Materials Fabrication

Fabrication. Samples were made in a three-step process of EBL, nickel die fabrication and hot embossing as has been published previously [Gadegaard et al., 2003; Dalby et al., 2004b].

Briefly, ZEP 520A coated silicon substrates were exposed in a Leica LBPG 5-HR100 beam-writer at 50 kV with an 80 nm spot in a hexagonal arrangement with 300 nm pitch.

Nickel dies were made directly from the patterned resist samples. A thin (50 nm) layer of Ni-V was sputter coated on the samples. This layer acted as an electrode in the subsequent electroplating process. The dies were plated to a thickness of ca. 300 μm.

Polymeric replicas, suitable for cell culture, of the original material were made in polymethylmethacrylate (PMMA) by hot embossing. This resulted in a final embossed diameter of 120 nm. Planar PMMA was used as a control (Fig. 1).

Cell Culture

Infinity^{TM} telomerase immortalised human fibroblasts (hTERT-BJ1, Clonetech) were seeded onto materials at a density of 1×10^4 cells/ml in complete medium. The medium used was 71% Dulbeccos Modified Eagles Medium (DMEM) (Sigma, UK), 17.5% Medium 199 (Sigma), 9% foetal calf serum (FCS) (Life Technologies, UK), 1.6% 200 mM L-glutamine (Life Technologies) and 0.9% 100 mM sodium pyruvate (Life Technologies). The cells were incubated at 37°C with a 5% CO_2 atmosphere, and the medium was changed regularly.

Cytoskeletal Poisoning

In sections where poisoning was used, the following protocols apply. MFs were poisoned for 10 min with 10 μM cytochalasin B. MTs were poisoned for 10 min with 1 μg/ml of colchicine. IFs were dissolved for 60 min with 4 mM acrylamide.

Cytoskeletal Observation

After 4 days of culture, the cells on the test materials were fixed in 4% formaldehyde/PBS,

with 1% sucrose at 37°C for 15 min. Once fixed, the cells were stained for immunofluorescence as has been previously described [Dalby et al., 2004a]. Briefly, the cells were permeablised (10.3 g sucrose, 0.292 g NaCl, 0.06 g $MgCl_2$, 0.476 g HEPES buffer, 0.5 ml Triton X, in 100 ml water, pH 7.2) and stained using phalloidin and primary monoclonal antibodies for vimentin and tubulin (V9 and tub 2.1, respectively, Sigma). A biotinylated anti-mouse secondary antibody and a FITC-streptavidin tertiary layer were then used (Vector Laboratories, UK). Nuclei were counterstained with DAPI.

Nucleoskeletal Observation

After 4 days of culture, the cells on the test materials were fixed, permeablised and blocked as above. Monoclonal anti-lamin B (1:50 in PBS/BSA, NA12, Calbiochem, UK) or A/C (1:50 in PBS/BSA, JOL 3, Insight Biotech, UK) was added at 37°C for 1 h. For Lamin B staining, cytoskeleton was simultaneously stained for using either phalloidin-rhodamine or phalloidin-Alexa 350 (1:50 in PBS/BSA, both Invitrogen, UK) and polyclonal primary antibodies for vimentin or tubulin (1:150 in PBS/BSA, V4630 and T220, respectively, both Sigma). After washing, a biotinylated anti-mouse antibody was added (1:50 in PBS/BSA, Vector Laboratories) for 1 h (37°C) followed by washing (NOTE: An anti-rabbit, TRITC conjugated, secondary was used for cytoskeletal labelling). A FITC conjugated streptavidin third layer was next added (1:50 in 1% BSA/PBS, Vector Laboratories at 4°C for 30 min).

Transmission Electron Microscopy

After 4 weeks of culture, the cells were fixed with 2% paraformaldehyde (Agar, UK)/PBS for 1 h at 37°C. Cells were postfixed with 1% osmium tetroxide, dehydrated in alcohols to 100%. Next, the samples were embedded in LR white medium resin (Agar) and polymerised at 60°C for 18 h. Ultrathin sections were then cut. The sections were blocked with PBS/BSA for 10 min and then a monoclonal anti-vinculin antibody (1:50, h-vin-1antibody, Sigma) was added for 2 h. After washing, a secondary 10 nm gold colloid conjugated anti-mouse antibody (Aurion, Netherlands) was added for 2 h. After washing, the samples were stained with uranyl acetate (2% aq.) and lead citrate, and viewed with a LEO 912 AB TEM.

Morphological & Adhesion Quantification

After 4 days of culture, the cells were fixed, permeablised and blocked as above before addition of phalloidin-rhodamine at 37°C for 1 h. After washing in 0.5% Tween 20/PBS, the cells were counterstained with DAPI and fluorescent images captured. ImageJ (free download from NIH) was used to automatically calculate whole cell and nucleus areas. It should be noted that standardised illumination conditions were used throughout.

For focal adhesion quantification cells were cultured without fresh media for 4 days. After this period, complete media was added for 14 h, when complete media with 10 μM bromodeoxyuridine (BrdU) was added for 3 h before fixation in 4% formaldehyde. From this point, similar protocols to those described in *Cytoskeletal Observation* were used, but with the substitution of monoclonal primary antibodies for BrdU (with DNAse, 1:50, Amersham, UK) and vinculin (1:50, h-vin1, Sigma). Vinculin adhesion staining only in S-phase cells (to remove arefact from different morphologies in different stages of cell-cycle) was then measured using Image J as above.

Centromere Labelling

After 4 days of culture, cells were fixed for 5 min in 3:1 methanol:glacial acetic acid. After fixation, the cells were dehydrated in 70, 90 and 100% ethanol (2 min 2× for each grade). Next, the cells were placed in 0.1% pepsin for 5 min before washing with 2× SSC and dehydrating for a second time. After dehydration, the cells were baked at 65°C for 1 h.

Biotin conjugated probes for centromeres of Ch 3 and Ch 11 (CamBio, UK) was warmed to 65°C for 5 min. The probes (pooled to the desired amount, 10 μl per sample) were next denatured at 80°C for 10 min and allowed to preanneal at 37°C for 10 min.

After baking, the cell preparations were denatured in 70% formamide/2× SSC for 2 min before quenching in ethanol and repeating the dehydration step. The denatured, preannealed probe was then added to the cells, a cover slip placed on top and hybridised at 37°C overnight. Labelling and amplification with FITC was performed the next day according to manufacturers protocol using an amplification kit (CamBio). Nuclei were counterstained with propridium iodide prior to viewing.

Statistics

All results were observed to be skewed to the left and were thus $\log_2$ transformed before use of one-way ANOVA (Tukey) using SigmaStat® software.

cDNA Microarrays

Gene expression changes were detected by using cDNA microarrays. The arrays were printed with 1,718 human transcripts obtained from the Ontario Microarray Centre (http://www.microarrays.ca). Complete protocols for the generation of fluorescence labelled samples from whole cell RNA, hybridisation to DNA microarrays and data processing can be found at this website.

Briefly, cells were cultured on the control ($n = 5$) and hex ($n = 5$) for 21 days. At this point, the cells were lysed and total RNA was extracted using an Absolutely RNA kit (Stratagene, UK) according to manufacturers instructions. The RNA was amplified using an Affymetrix Gene Chip Amplification kit according to the supplied protocol. Five micrograms of RNA was used to make Alexa 555- or Alexa 647- (Invitrogen) labelled cDNA suing Superscript II reverse transcriptase (Invitrogen). Samples were prepared for hybridisation by combining fragmented salmon sperm DNA (0.5 μg/μl; Gibco BRL, UK) and yeast tRNA (0.5 μg/μl; Gibco BRL) in EasyHyb solution (Roche Diagnostics, UK). Samples were hybridised for 18 h at 37°C onto five cDNA microarrays. Arrays were next washed three times at 50°C with 0.1% (v/v) saline sodium citrate (SSC) containing 0.1% (v/v) SDS followed by one wash with 0.1% SSC alone. All five arrays were scanned to produce TIFF files using ScanArray scanner and software suite (Packard BioChip Technologies, Billerica, MA).

Log_2 normalised data generated by comparison of spot intensity between sample and control was then plotted to show general patterns of gene regulation.

RESULTS

Cell Adhesion

TEM observation of vinculin/cellular interaction with pits showed that the pits do alter fibroblast adhesion. As shown in Figure 2, highly ordered EBL structures, such as hex, cause low-adhesion of fibroblasts [Gallagher et al., 2002; Dalby et al., 2004b]. Here, adhesions were seen close to filopodia locating in-between the pits (Fig. 2A); as the cells came into closer contact with the surface, the contacts were seen to mature into focal adhesions on the planar areas (Fig. 2B). Areas of the cells in contact with the nanopits generally had no, or very low levels, of vinculin localisation (Fig 2C).

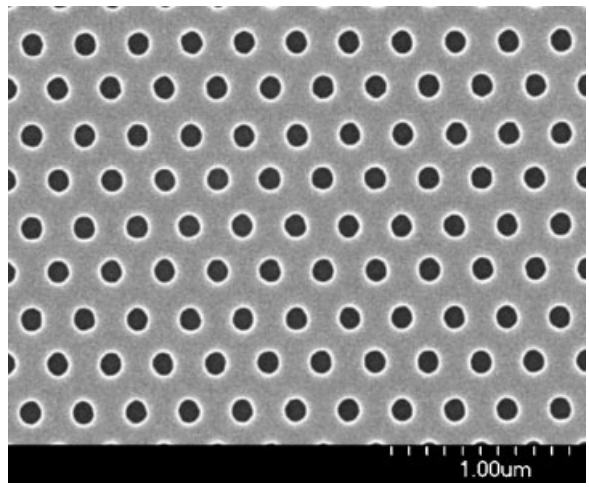

Fig. 1. Scanning electron micrograph of electron beam fabricated nanopits. Pits with hexagonal arrangement—diameter 100 nm, depth 100 nm, centre-centre spacing 300 nm.

Quantification of adhesion size and numbers showed that whilst the pattern of focal contact (FC, <2 μm), focal adhesion (FA, 2–5 μm) and fibrilar adhesion (FbA, >5 μm) remained similar, significantly fewer adhesions of each type were formed in cells on the hex symmetry compared to control.

As could be expected with the focal adhesions of a cell acting as anchoring points for the cytoskeleton, the topographically induced reduction in focal contact formation resulted in large changes in cytoskeletal organisation (Fig. 3) and cell morphology (Fig. 4A).

Morphology & Cytoskeleton

On planar control (Ra 1.17 nm over 10 μm), fibroblasts were seen to have well-organised MFs (Fig. 3A,B), MTs (Fig. 3A) and IFs (Fig. 3B) cytoskeletons. On hex, however, few stress fibres were observed (Fig. 3C,D), and the IFs were observed to be poorly defined and dense around the nucleus (Fig. 3D). MTs, however, remained well organised in cells on the EBL hex samples (Fig. 3C). This ties in with results from fibroblasts cultured on 160 nm high nanocolumns, whereby the features induced

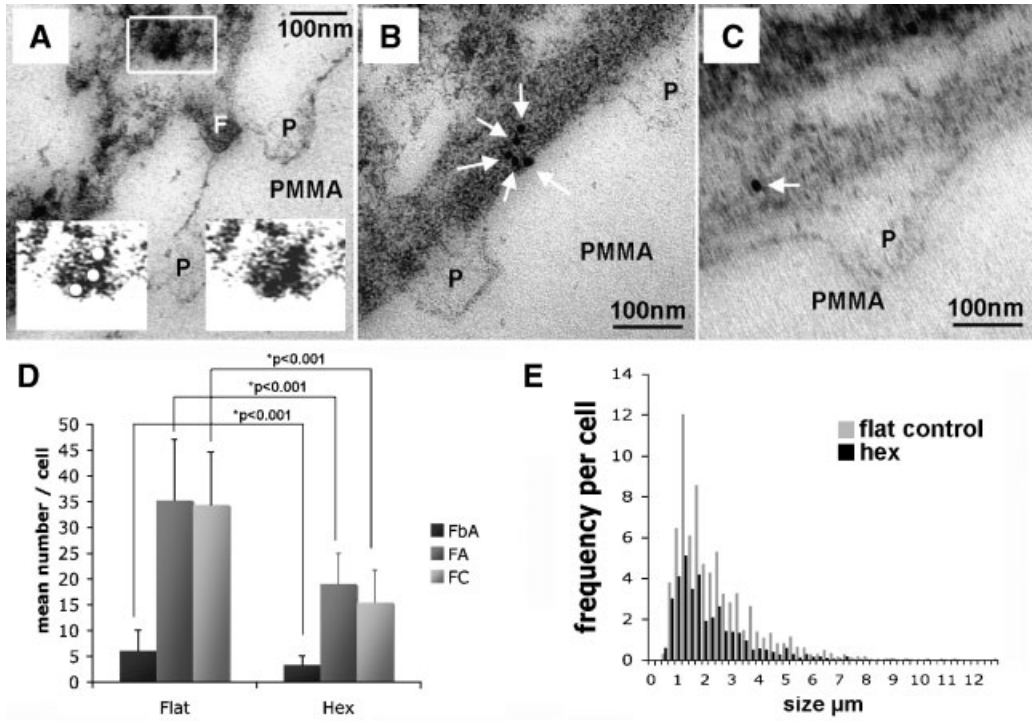

Fig. 2. Transmission electron microscopical images of fibroblasts cultured on nanopits immunogold stained for vinculin and adhesion size quantification. **A**: Filopodia (F) protruding from the underside of a fibroblast locating in-between pits (P). A nascent focal contact can be seen directly above the filopodia (boxed); insets are enhancements of the boxed original, one using red to pick out the gold particles. **B**: Focal contact (arrows) located in-between pits (P). **C**: Very limited (normally no) focal contact/adhesion (arrow) formation near pits (P). **D**: Graph showing mean number of focal adhesion (FA), focal contact (FC) and fibrilar adhesion (FbA) in cells on flat control and hex topographies (results are the mean ± SD). Adhesion numbers were seen to be significantly reduced in cells cultured on hex compared to those cultured on control (results are mean ± SD). **E**: Size distribution for fibrobasts cultured on flat control and hex topographies. The distribution was seen to be similar, but numbers reduced on hex compared to control (33 and 34 cells counted on flat and hex, respectively).

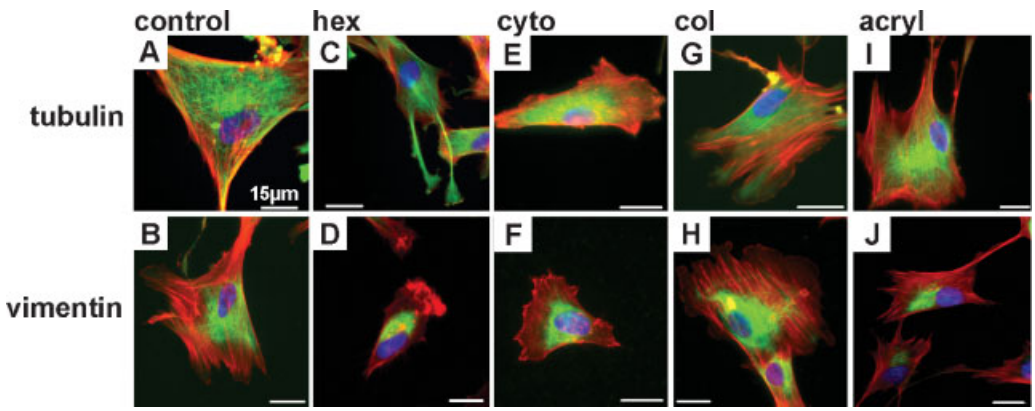

Fig. 3. Fluorescence images of fibroblast cytoskeletons on planar controls, hex nanotopography and with poisoned cytoskeletons. In all images, MFs are red and nuclei are blue. (**A**, **C**, **E**, **G**, **I**) MTs = green. (**B**, **D**, **F**, **H**, **J**) IFs = green. A, B: Cells on control were well spread with stress fibres, clearly organised MTs and distinct, radiating IFs. C, D: Cells on hex were poorly spread with diffuse MF's but well-ordered MTs and had IFs with a dense appearance close to the nucleus. E, F: Shows punctate MF cytoskeleton after culturing with cytochalasin, MT's and IF's remain organized. G, H: Shows diffuse MT staining with cells cultured with colchicine, MF's and IF's remain organized. I, J: Shows poorly organized IF staining after culture with acrylaminde, MF's and MT's remain clearly organized.

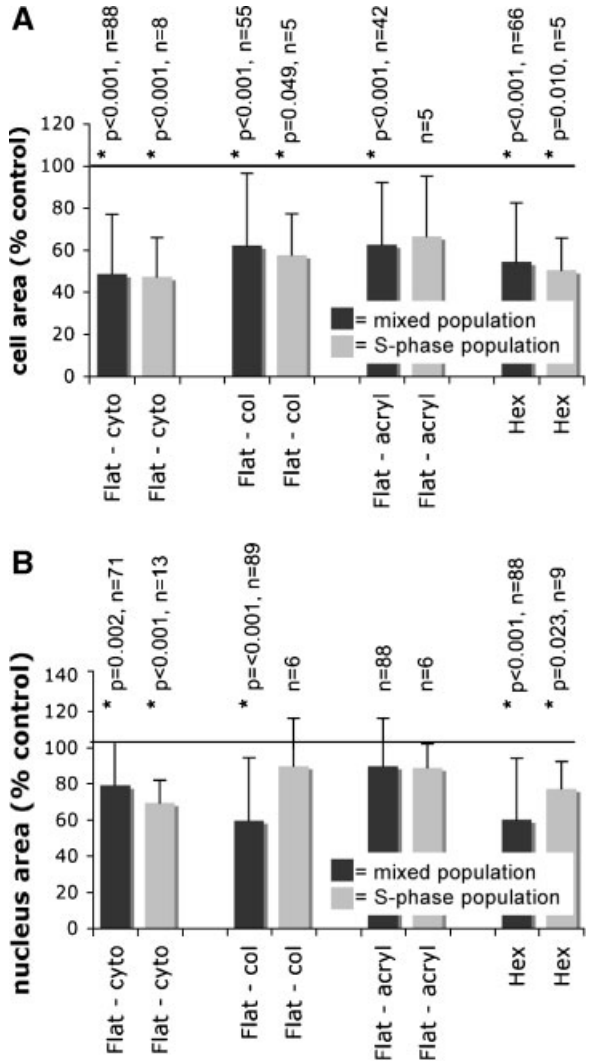

Fig. 4. Graphs of cell and nuclei areas in mixed phase and S-phase populations. For (**A**) and (**B**) cyto = cytochalasin D to poison MF's, col = colchicine to poison MT's and acryl = acrylamide to poison IF's (A). Graph showing whole cell areas. S-phase and mixed phase trends are a close match. Culturing cells on hex and poisoning of MF's leads to the largest reduction in cell areas. B: Graph showing nuclei areas, S-phase and mixed phase trends are a reasonable match and again shows that culturing cells on hex and poisoning of MF's leads to the largest reduction in nuclei areas. Results are mean ± SD.

an endocytosis-like response and the cells attempt to internalise the nanostructure [Dalby et al., 2004a]. Poisons for each cytoskeletal type were also used (Fig. 3E–J). Cytochalasin treatment induced the largest changes (Fig. 3E,F) producing cells of comparable morphology to those cultured on hex. Colchicine and acrylamide treatments produced well spread cells with clear stress fibres (Fig. 3G–J).

The first step in assessing direct mechanotransduction is to observe changes in cellular morphology. Figure 4A shows measurements of cell spreading (area) in mixed phase and S-phase only populations. S-phase populations were used to confirm that results for mixed phase area (with larger samples sizes) were true, and not effects of different stages of cell-cycle due to changes in proliferation (i.e. shifts from G1 to G2 populations). In order to consider how the individual cytoskeletons may affect direct mechanotransduction, as well as considering the combined effects of hex, cytoskeletal inhibitors were again used as shown in Figure 3.

Trends in cell spreading in the mixed populations were seen to follow closely those of the S-phase-only populations (Fig. 4A). Poisoning of MFs had the largest effect on cell spreading. Poisoning of MTs and IFs reduced cell spreading to an extent. Cells cultured on the hex nanotopography reduced spreading to a similar extent as with MF poisoning.

For direct mechanotransduction to occur, these effects must be seen in the cell nucleus. Again, results for mixed phase nuclei areas have been compared to those for S-phase nuclei areas and the fit is reasonable (Fig. 4B). As with whole cell areas, the largest changes were observed in cells with MFs poisoned and in cells cultured on hex. Results for MTs showed a significant reduction in nuclei areas, but not as great. Results for IFs, whilst showing decreased areas, failed to show statistical differences.

Comparison of results for whole cell and nuclear morphology tie in with each other and suggest direct mechanotransduction has occurred due to nanotopography.

Nucleoskeleton

Our results for lamins B and A/C fit with the results of Dahl et al. The larger nuclei (under most tension) have a diffuse lamina network (Fig. 5A,C,E,G), whereas cells cultured on the hex sample have a dense lamina network (Fig. 5B,D,F,K). As has been discussed, Figure 5A,B shows MF stress fibres passing over the nuclei, Figure 5C,D shows the MT organizing centre located next to the nucleus and Figure 5E,F shows IF connecting all around the periphery of the nucleus. Results for lamin B have also been considered with cytoskeletal poisoning (Fig. 5G–K). As with observations of morphology, results for cells cultured on the hex show similarities for MF poisoned cells,

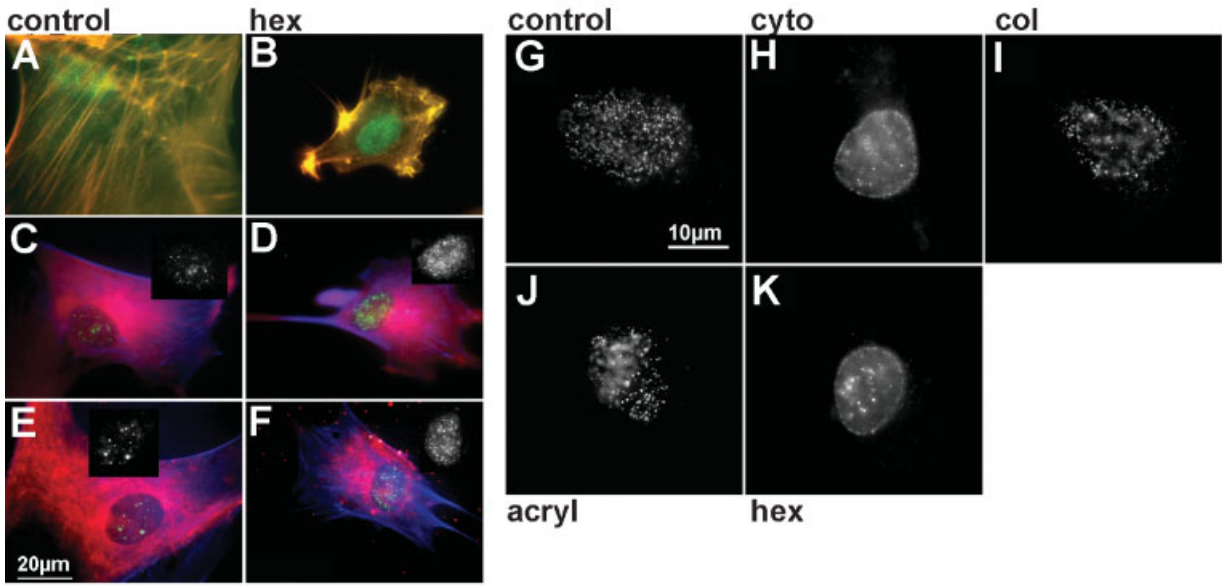

Fig. 5. Lamin B and A/C nucleoskeletons in fibroblasts cultured on control and hex materials. **A–F**: Lamin B (green in all images) and cytoskeletons. A, B: Lamin B and MF's (yellow) on control and hex, respectively. On control, cells were well-spread with clear stress fibres passing over the nuclei and a diffuse lamin B appearance. On hex, cells were poorly spread with dense nucleoskeleton. C, D: Lamin B, MF's (blue) and MT's (red) on control and hex, respectively. Again, lamin B appeared diffuse on control and dense on hex (see black and white insets also). MT's were well organised on both materials with the organising centre clearly visible next to the nucleus. E, F: Lamin B, MF's (blue) and IF's (red) on control and hex, respectively. Again, lamin B appeared diffuse on control and dense on hex (see black and white insets also). IF's were clearly organised on control, but had a dense appearance close to the nuclei on hex. **G–K**: Lamin A/C. G: Lamin A/C on control had a diffuse appearance. H, K: Lamin A/C had a very dense appearance in cells cultured with cytochalasin D (cyto) to poison MF's and on hex. I, J: Lamin A/C had an intermediate appearance in cells cultured with colchicine (col) to poison MT's and acrylamide (acryl) to poison IF's.

whereas the results for MT and IF cells are in between the strained nuclei and the relaxed nuclei results.

Interphase Chromosome Positioning

Here, we test this and the hypothesis of relative consistency of Ch positioning in the interphase nuclei by looking at centromeres of G2 Ch 3. Figure 6A shows results for Ch 3 measurements in cells on control, hex and with poisoned cytoskeletons. As with previous results, the largest changes are noted with MF poisoning and with cells cultured on hex. The results for MT and IF poisoning show intermediate states, but are not statistically significant. Figure 6B shows that the relative position of Ch 11 is also changed and Figure 6C shows images of the centromeres in G2 nuclei.

Gene Regulation

Normalised array data shows broad down-regulation of genes in fibroblasts cultured on hex compared to those on control (Fig. 7).

DISCUSSION

It has been known for many years that cells will react to the shape of their environment [Carrel and Burrows, 1911; Weiss and Garber, 1952; Curtis and Varde, 1964]. More recent reports have shown morphological [Oakley and Brunette, 1993; Chou et al., 1995; Andersson et al., 2003; Hamilton and Brunette, 2005] and genomic [Dalby et al., 2002, 2003] responses in cells cultured on fabricated substrates. These surfaces range from the μm scale down to the nm scale as technology has advanced [Wilkinson et al., 2002; Gadegaard et al., 2003].

It is clear that the natural environment of a cell will have topography derived from neighbouring cells at the μm scale and protein folding and banding (such as the 64 nm repeat pattern of collagen [Curtis and Wilkinson, 2001]) at the nm level. These considerations are in addition to the mm and cm scale of the whole tissue in which the cells are located. Thus, in biomaterials and tissue engineering, the topography of an implant or scaffold may be a powerful tool in

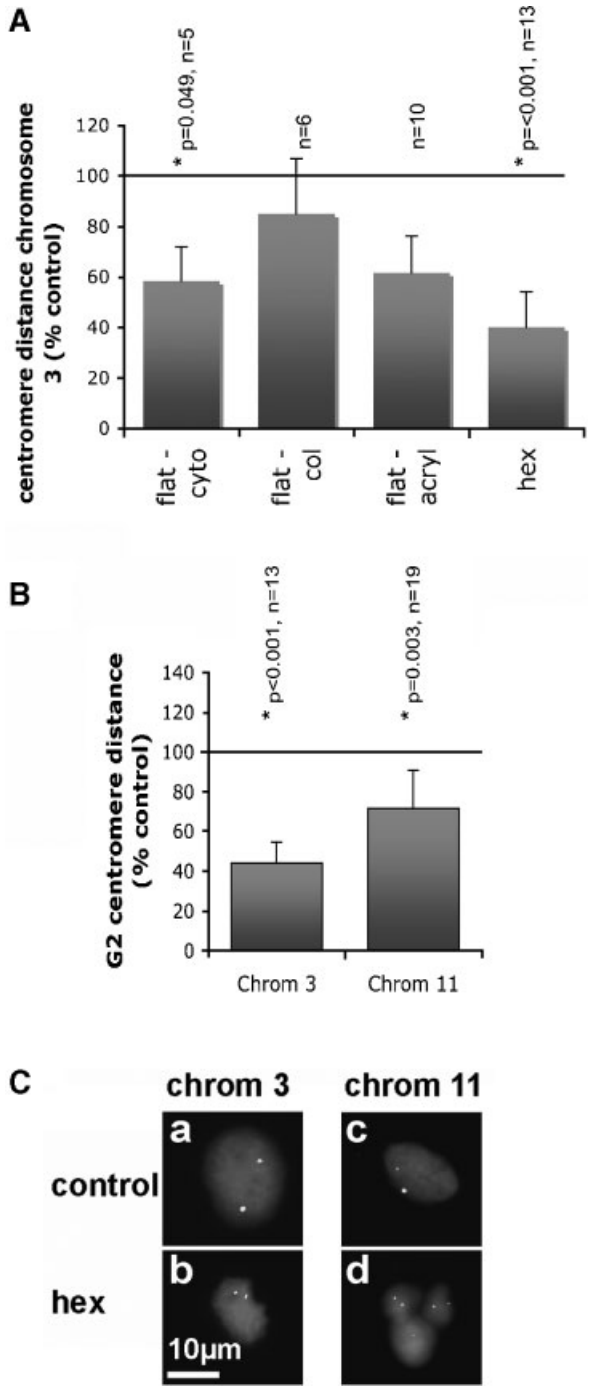

Fig. 6. Centromere analysis. **A**: Graph showing G2 interphase centromere measurements for chromosome 3. Culturing cells with cytochalasin D (cyto) to poison MF's and on hex causes the largest changes in measured distance. Cells cultured with colchicine (col) to poison MT's and acrylamide (acryl) to poison IF's had intermediate changes in relative positioning. **B**: Graph showing G2 interphase centromere analysis for chromosomes 3 and 11. **C**: Images of cell nuclei with G2 interphase centromere pairs for Chromosomes 3 and 11 shown as bright dots.

eliciting desired responses from cells to augment tissue repair and regeneration.

However, it is not clear how cells respond to topography, especially at the nanolevel. The first consideration is changes in surface energy at the fluid/solid interface resulting from nanotopography. Texture can produce "superhydrophobic" and "superhydrophilic" surfaces—as well as states of hydrophobicity and hydrophilicity in-between. Most highly organised nanotopographies are hydrophobic, that is if a droplet of water is placed on these surfaces, it will remain rounded and roll off rather than spreading into a thin film. This phenomenon has been termed the "Lotus effect" after the water repellent leaves of the lotus plant (*Nelumbo nucifera*) [Furstner and Barthlott, 2005]. These leaves exhibit a double-structured roughness, where submicrometric wax crystals cover a larger micrometric structure.

A recent study calculating the contact angle of various EBL nanostructures showed such ordered and nanoscale arrays can range from hydrophobic to "superhydrophobic" depending on properties such as aspect ratio [Martines et al., 2005]. Work from the Kasemo group has demonstrated for many years now the importance of considering properties of surface chemistry and physics, of which wetability is one [Kasemo and Lausmaa, 1988; Zhdanov and Kasemo, 2000]. Thus, it is probable that at the nanolevel, the hex surface becomes repellent to the proteins required for cellular adhesion.

The reduction in adhesive protein adsorbtion may detrimentally affect the ability of cells to form adhesions, especially the larger fibrilar adhesions. Integrin gathering is also essential for the formation of contractile stress fibres. Certainly, here, the fibroblasts cultured on hex had many less adhesions and reduced cytoskeletal organisation.

The results for MFs and hex are intriguing as they show the largest reductions in cell and nucleus area. This fits with Ingber's [1993] theory of tensegrity. In order to have tensegrity, MFs are required to generate prestress. Thus, inability to form structured MF networks would result in lack of tensegrity. Cells tend to operate with high levels of redundancy, and thus the results for compromised MTs and MFs are not surprising. Poisoning for such short periods of time appeared not to result in total depolymerisation, rather partial. Thus, as long as prestress could be applied, the tensegrity structures

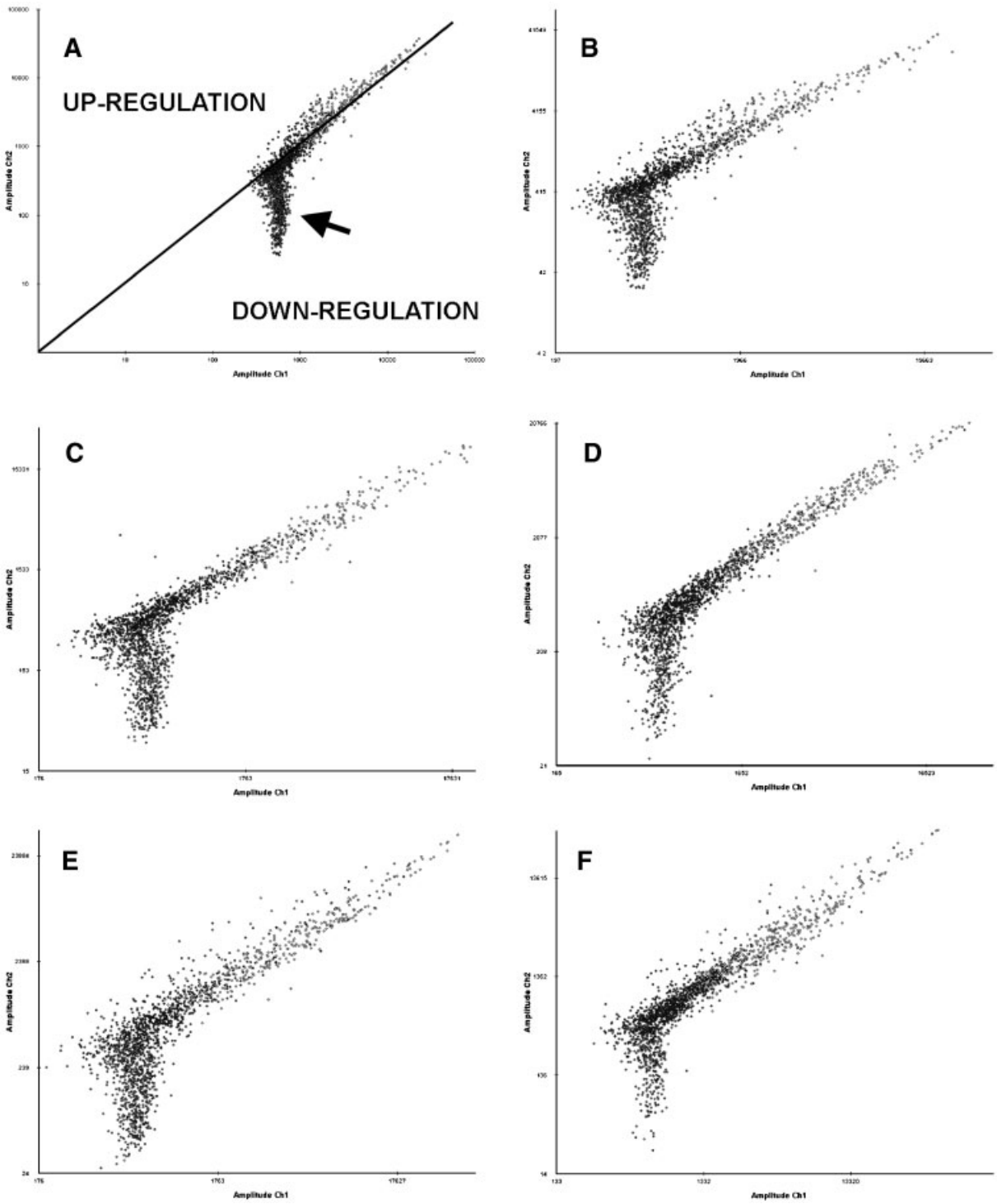

Fig. 7. Graphs showing gene expression profiles. **A**: Zoomed-out graph for array 1 showing the line separating up- and downregulations and the individual genes as scatter points. **B–F**: Zoomed-in scatter plots for arrays 1–5, respectively. In all the graphs note that most of the changes in regulation fit into the downregulation categories, especially when most of the points lying close to the line would be considered insignificant changes.

could operate with reduced function. Also, once the prestress is removed, no further mechanical compromise was observed (as with hex where both MF and IF organisation are reduced).

IFs are the only cystoskeletal proteins to connect directly with the nucleus, forming a continuous network with the nucleoskeletal filaments hence linking the nuclear membrane directly with the plasma membrane [Maniotis et al., 1997b; Georgatos and Blobel, 1987]. MFs pass over the nucleus and MTs are organised close to the nucleus. MFs and MTs, however, are closely associated with focal adhesions, again suggesting an integrated cytoskeletal network with some order required to propagate mechanical signals to the nucleus.

The Young's moduli of the individual cytoskeletons would suggest that they would have to transduce mechanical signals via tension as perhaps only bundled MFs could transmit compressive force. Certainly here, cells on the planar control are well spread with large nuclei, whereas cells on hex are less spread with smaller nuclei. Whilst it could be conceived that a well-organised cytoskeleton could pull on a nucleus, increasing its size, it is hard to imagine that a poorly organised cytoskeleton could compress a nucleus. Thus, it is likely that the large control nuclei are under tensile strain, whereas the nuclei of cells on hex are merely relaxed. This fits well with results by Dahl et al. [2004]. They showed the nuclear lamina network to be highly elastic, but to have a compression limit, suggesting that the lamins act as a molecular shock absorber. Their results indicate that the lamina forms a shell of interconnected rods, that is extensible but limited in compressibility.

Other studies have also provided evidence that IFs can transmit stress signals to chromatin [Bloom et al., 1996] and that in reaction to tension, the IFs re-orientate leading to nuclear distortion and nucleoli rearrangement along the applied axis [Maniotis et al., 1997b]. This signalling could happen through cytoskeletal IF interaction with nucleoskeletal IFs and be transmitted to DNA via the close relationship of lamins and chromatin [Bloom et al., 1996; Goldman et al., 2002].

Wang and Suo [2005] write that this type of 'action at a distance' force propogation, that is from the cell membrane to the nucleus, disagrees with models that regard the cell as a homogeneous body [Gudi et al., 1998; Heidemann et al., 1999; Mijailovich et al., 2002]. These theories predict that locally applied force (e.g. on a focal adhesion) decays over a short distance. Wang and Suo suggest that long-distance propagation originates from cellular inhomogenity, with stiff MF bundles within a compliant cytoskeletal network. They further suggest that it is the large ratio of prestress and modulus of the actin bundles (an individual MF has a modulus of approximately 1×10^9 Pa) compared to that of the cystoskeletal network (100–1,000 Pa) [Janmey et al., 1991; Gittes et al., 1993] that allows propogation. They further speculate that, as MTs are associated with MFs in migrating cells, MTs stiffened by IFs together with MF bundles may function as an integrated mechanical unit; this is consistent with the theory of tensegrity. They demonstrate their theories by applying local forces to cells using RGD coated magnetic microbeads attached to cell adhesions and then applying torque. Observations of changes in cytoskeletal [Hu et al., 2003; Wang and Suo, 2005] and nuclear [Hu et al., 2004] morphology were then made.

With regards issues of tensegrity and percolation, it would seem sensible to argue for a flexible system where IFs as well as MFs can form the tensile element of a tensegrity structure, as this would agree with cells natural propensity for redundancy in signalling. It is also possible, and seems likely, that both states co-exist and that tensegrity structures form in areas where support is required and forces are applied. In fact, cellular tensegrity could be considered to be organised percolation structures and may be best considered as application of tensegrity principles, rather than pure, structural, tensegrity with defined numbers of struts etc.

Thus, it is postulated that events such as adhesion, proliferation and differentiation can be enhanced/inhibited by nanotopography and that a significant pathway of signal transduction is direct mechanotransduction through the cytoskeleton and than via the nucleoskeleton directly to the interphase DNA. It is perhaps tempting to speculate that this could then alter the probability of gene transcription. These results fit well with comments by Forgacs who stated that perhaps the cell is just part of a larger percolation environment, with collagen fibres throughout the matrix linking to an interconnected cytoskeleton via adhesions. We

extend this to the DNA and postulate that direct mechanical linking with the matrix leads to changes in gene positioning and hence regulation. This is in strong agreement with the topographical model of the nucleus [Kurz et al., 1996; Sun et al., 2000; Cremer and Cremer, 2001; Scheuermann et al., 2004; Murmann et al., 2005] and may help explain tissue-dependent gene regulation.

Getzenberg [1994] commented that tissue-specific gene expression is intriguing as regulation by single transcription factors cannot be explained simply by DNA sequence. Getzenberg suggests the three-dimensional organisation of the genome, structural components of the nucleus and nuclear matrix in different tissues may alter specific gene regulation. Certainly, topographical induction of changes in cell spreading has lead to changes in gene profile.

Recent evidence has shown that nm topography can influence osteoprogenitor differentiation in to nodule forming osteoblasts without the need for osteogenic medium supplemements [Dalby et al., 2005, 2006a,b]. This may also help explain how mechanical preconditioning of cells in collagen (or similar) gels aids tissue engineering preconditioning, that is mechanical stimulation of cells within a percolation environment [Knight et al., 2002; Berry et al., 2003].

A further experiment with great merit would be to compare these results to those from an environment patterned with adhesion suppressing chemistry produced by, for example microcontact printing.

ACKNOWLEDGMENTS

M.J.D. is a BBSRC David Phillips Fellow and this research was funded though his fellowship. N.G. is a Royal Society of Edinburgh Research Fellow. A.S.G. is supported by EC grant NANOCUES NMP-STREP 2004 505868-1. The authors especially thank Dr. Mathis Riehle for guidance and use of his fluorescence microscope. We also thank the IBLS Integrated Microscopy Facility and the Sir Henry Wellcome Functional Genomics Facility.

REFERENCES

Andersson AS, Olsson P, Lidberg U, Sutherland D. 2003. The effects of continuous and discontinuous groove edges on cell shape and alignment. Exp Cell Res 288:177–188.

Ball P. 2001. Life's lessons in design. Nature 409:413–416.

Berry CC, Shelton JC, Bader DL, Lee DA. 2003. Influence of external uniaxial cyclic strain on oriented fibroblast-seeded collagen gels. Tissue Eng 9:613–624.

Bloom S, Lockard VG, Bloom M. 1996. Intermediate filament-mediated stretch-induced changes in chromatin: A hypothesis for growth initiation in cardiac myocytes. J Mol Cell Cardiol 28:2123–2127.

Carrel A, Burrows M. 1911. Culture in vitro of malignant tumors. J Exp Med 12:571–575.

Charras GT, Horton MA. 2002. Single cell mechanotransduction and its modulation analyzed by atomic force microscope indentation. Biophys J 82:2970–2981.

Chou L, Firth JD, Uitto VJ, Brunette DM. 1995. Substratum surface topography alters cell shape and regulates fibronectin mRNA level, mRNA stability, secretion and assembly in human fibroblasts. J Cell Sci 108(Pt 4):1563–1573.

Cremer T, Cremer C. 2001. Chromosome territories, nuclear architecture and gene regulation in mammalian cells. Nat Rev Genet 2:292–301.

Curtis ASG, Varde M. 1964. Control of cell behaviour: Topological factors. J Nat Cancer Res Inst 33:15–26.

Curtis ASG, Wilkinson CDW. 2001. Nanotechniques and approaches in biotechnology. Trends Biotechnol 19:97–101.

Dahl KN, Kahn SM, Wilson KL, Discher DE. 2004. The nuclear envelope lamina network has elasticity and a compressibility limit suggestive of a molecular shock absorber. J Cell Sci 117:4779–4786.

Dalby MJ, Yarwood SJ, Riehle MO, Johnstone HJ, Affrossman S, Curtis AS. 2002. Increasing fibroblast response to materials using nanotopography: Morphological and genetic measurements of cell response to 13-nm-high polymer demixed islands. Exp Cell Res 276:1–9.

Dalby MJ, Riehle MO, Yarwood SJ, Wilkinson CD, Curtis AS. 2003. Nucleus alignment and cell signaling in fibroblasts: Response to a micro-grooved topography. Exp Cell Res 284:274–282.

Dalby MJ, Berry CC, Riehle MO, Sutherland DS, Agheli H, Curtis AS. 2004a. Attempted endocytosis of nano-environment produced by colloidal lithography by human fibroblasts. Exp Cell Res 295:387–394.

Dalby MJ, Gadegaard N, Riehle MO, Wilkinson CD, Curtis AS. 2004b. Investigating filopodia sensing using arrays of defined nano-pits down to 35 nm diameter in size. Int J Biochem Cell Biol 36:2015–2025.

Dalby MJ, McCloy D, Robertson M, Wilkinson CDW, Oreffo ROC. 2006. Osteoprogenitor response to defined topographies with nanoscale depths. Biomaterials 27:1306–1315.

Dalby MJ, McCloy D, Robertson M, Agheli H, Sutherland D, Affrossman S, Oreffo RO. 2006a. Osteoprogenitor response to semi-ordered and random nanotopographies. Biomaterials 27:2980–2987.

Dalby MJ, McCloy D, Robertson M, Wilkinson CDW, Oreffo ROC. 2006b. Osteoprogenitor response to defined topographies with nanoscale depths. Biomaterials 27:1306–1315.

DuPraw E. 1965. The organization of nuclei and chromosomes in honeybee embronic cells. Proc Natl Acad Sci USA 53:161–168.

Fey EG, Wan KM, Penman S. 1984. Epithelial cytoskeletal framework and nuclear matrix-intermediate filament scaffold: Three-dimensional organization and protein composition. J Cell Biol 98:1973–1984.

Forgacs G. 1995. On the possible role of cytoskeletal filamentous networks in intracellular signaling: An approach based on percolation. J Cell Sci 108(Pt 6): 2131–2143.

Fuller B. 1961. Tensegrity. Portfolio Artnews Annu 4: 112–127.

Furstner R, Barthlott W. 2005. Wetting and self-cleaning properties of artificial superhydrophobic surfaces. Langmuir 21:956–961.

Gadegaard N, Thoms S, MacIntyre DS, McGhee K, Gallagher J, Casey B, Wilkinson CDW. 2003. Arrays of nano-dots for cellular engineering. Microelectronic Eng 67–68:162–168.

Gallagher JO, McGhee KF, Wilkinson CDW, Riehle MO. 2002. Interaction of animal cells with ordered nanotopography. IEEE Trans Nanobiosci 1:24–28.

Georgatos SD, Blobel G. 1987. Lamin B constitutes an intermediate filament attachment site at the nuclear envelope. J Cell Biol 105:117–125.

Getzenberg RH. 1994. Nuclear matrix and the regulation of gene expression: Tissue specificity. J Cell Biochem 55: 22–31.

Gittes F, Mickey B, Nettleton J, Howard J. 1993. Flexural rigidity of microtubules and actin filaments measured from thermal fluctuations in shape. J Cell Biol 120:923–934.

Goldman RD, Gruenbaum Y, Moir RD, Shumaker DK, Spann TP. 2002. Nuclear lamins: Building blocks of nuclear architecture. Genes Dev 16:533–547.

Gudi SR, Lee AA, Clark CB, Frangos JA. 1998. Equibiaxial strain and strain rate stimulate early activation of G proteins in cardiac fibroblasts. Am J Physiol 274:C1424–C1428.

Hamilton DW, Brunette DM. 2005. "Gap guidance" of fibroblasts and epithelial cells by discontinuous edged surfaces. Exp Cell Res 309:429–437.

Heidemann SR, Kaech S, Buxbaum RE, Matus A. 1999. Direct observations of the mechanical behaviors of the cytoskeleton in living fibroblasts. J Cell Biol 145:109–122.

Heslop-Harrison JS. 2000. Comparative genome organization in plants: From sequence and markers to chromatin and chromosomes. Plant Cell 12:617–636.

Heslop-Harrison JS. 2003. Planning for remodelling: Nuclear architecture, chromatin and chromosomes. Trends Plant Sci 8:195–197.

Heslop-Harrison JS, Leitch AR, Schwarzacher T. 1993. The physical organisation of interphase nuclei. In: Heslop-Harrison JS, Flavell RB, (editors). The Chromosome. Oxford: Bios. pp 221–232.

Hoskins GC. 1965. Electron microscopic observations of human chromosomes isolated by micrurgy. Nature 207:1215–1216.

Hoskins GC. 1968. Sensitivity of microsurgically removed chromosome spinadal fibres to enzyme disruption. Nature 217:748–750.

Hotani H, Miyamoto H. 1990. Dynamic features of microtubules as visualized by dark-field microscopy. Adv Biophys 26:135–156.

Hu S, Chen J, Fabry B, Numaguchi Y, Gouldstone A, Ingber DE, Fredberg JJ, Butler JP, Wang N. 2003. Intracellular stress tomography reveals stress focusing and structural anisotropy in cytoskeleton of living cells. Am J Physiol Cell Physiol 285:C1082–C1090.

Hu S, Eberhard L, Chen J, Love JC, Butler JP, Fredberg JJ, Whitesides GM, Wang N. 2004. Mechanical anisotropy of adherent cells probed by a three-dimensional magnetic twisting device. Am J Physiol Cell Physiol 287:C1184–C1191.

Ingber DE. 1993. Cellular tensegrity: Defining new rules of biological design that govern the cytoskeleton. J Cell Sci 104(Pt 3):613–627.

Ingber DE. 2003a. Tensegrity I. Cell structure and hierarchical systems biology. J Cell Sci 116:1157–1173.

Ingber DE. 2003b. Tensegrity II. How structural networks influence cellular information processing networks. J Cell Sci 116:1397–1408.

Janmey PA. 1991. Mechanical properties of cytoskeletal polymers. Curr Opin Cell Biol 3:4–11.

Janmey PA, Euteneuer U, Traub P, Schliwa M. 1991. Viscoelastic properties of vimentin compared with other filamentous biopolymer networks. J Cell Biol 113:155–160.

Kasemo B, Lausmaa J. 1988. Biomaterial and implant surfaces: A surface science approach. Int J Oral Maxillofac Implants 3:247–259.

Katsumi A, Orr AW, Tzima E, Schwartz MA. 2004. Integrins in mechanotransduction. J Biol Chem 279: 12001–12004.

Knight MM, van de Breevaart Bravenboer J, Lee DA, van Osch GJ, Weinans H, Bader DL. 2002. Cell and nucleus deformation in compressed chondrocyte-alginate constructs: Temporal changes and calculation of cell modulus. Biochim Biophys Acta 1570:1–8.

Kurz A, Lampel S, Nickolenko JE, Bradl J, Benner A, Zirbel RM, Cremer T, Lichter P. 1996. Active and inactive genes localize preferentially in the periphery of chromosome territories. J Cell Biol 135:1195–1205.

MacKintosh FC, Kas J, Janmey PA. 1995. Elasticity of semiflexible bipolymer networks. Phys Rev Lett 75: 4425–4428.

Maniotis AJ, Bojanowski K, Ingber DE. 1997a. Mechanical continuity and reversible chromosome disassembly within intact genomes removed from living cells. J Cell Biochem 65:114–130.

Maniotis AJ, Chen CS, Ingber DE. 1997b. Demonstration of mechanical connections between integrins, cytoskeletal filaments, and nucleoplasm that stabilize nuclear structure. Proc Natl Acad Sci USA 94:849–854.

Martines E, Seunarine K, Morgan H, Gadegaard N, Wilkinson CDW, Riehle MO. 2005. Superhydrophobicity and superhydrophilicity of regular nanopatterns. Nanoletters 5:2097–2103.

Mijailovich SM, Kojic M, Zivkovic M, Fabry B, Fredberg JJ. 2002. A finite element model of cell deformation during magnetic bead twisting. J Appl Physiol 93:1429–1436.

Mizushima-Sugano J, Maeda T, Miki-Noumura T. 1983. Flexural rigidity of singlet microtubules estimated from statistical analysis of their contour lengths and end-to-end distances. Biochim Biophys Acta 755:257–262.

Murmann AE, Gao J, Encinosa M, Gautier M, Peter ME, Eils R, Lichter P, Rowley JD. 2005. Local gene density predicts the spatial position of genetic loci in the interphase nucleus. Exp Cell Res 311:14–26.

Oakley C, Brunette DM. 1993. The sequence of alignment of microtubules, focal contacts and actin filaments in fibroblasts spreading on smooth and grooved titanium substrata. J Cell Sci 106:343–354.

Scheuermann MO, Tajbakhsh J, Kurz A, Saracoglu K, Eils R, Lichter P. 2004. Topology of genes and nontranscribed sequences in human interphase nuclei. Exp Cell Res 301: 266–279.

Shafrir Y, Forgacs G. 2002. Mechanotransduction through the cytoskeleton. Am J Physiol Cell Physiol 282:C479–486.

Sun HB, Shen J, Yokota H. 2000. Size-dependent positioning of human chromosomes in interphase nuclei. Biophys J 79:184–190.

Volpi EV, Chevret E, Jones T, Vatcheva R, Williamson J, Beck S, Campbell RD, Goldsworthy M, Powis SH, Ragoussis J, Trowsdale J, Sheer D. 2000. Large-scale chromatin organization of the major histocompatibility complex and other regions of human chromosome 6 and its response to interferon in interphase nuclei. J Cell Sci 113(Pt 9):1565–1576.

Wang N, Suo Z. 2005. Long-distance propagation of forces in a cell. Biochem Biophys Res Commun 328:1133–1138.

Weiss P, Garber B. 1952. Shape and movement of mesenchyme cells as functions of the physical structure of the medium. Proc Natl Acad Sci USA 38:264–280.

Wilkinson CDW, Riehle M, Wood M, Gallagher J, Curtis ASG. 2002. The use of materials patterned on a nano- and micro-metric scale in cellular engineering. Mater Sci Eng 19:263–269.

Williams RR, Broad S, Sheer D, Ragoussis J. 2002. Subchromosomal positioning of the epidermal differentiation complex. EDC) in keratinocyte and lymphoblast interphase nuclei. Exp Cell Res 272:163–175.

Zhdanov VP, Kasemo B. 2000. Ordering of adsorbed proteins. Proteins 40:539–542.